

# EXPERIMENTS IN THE MACHINING OF ICE AT NEGATIVE RAKE ANGLES

By D.K. LIEU

(Advisory Engineer, Sperry Corporation, Santa Clara, California 95051, U.S.A.)

and C.D. MOTE, JR.

(Department of Mechanical Engineering, University of California, Berkeley, California 94720, U.S.A.)

**ABSTRACT.** The cutting force components and the cutting moment on the cutting tool were measured during the orthogonal machining of ice with cutting tools inclined at negative rake angles. The variables included the cutting depth ( $< 1$  mm), the cutting speed ( $0.01 \text{ m s}^{-1}$  to  $1 \text{ m s}^{-1}$ ), and the rake angles ( $-15^\circ$  to  $-60^\circ$ ). Results of the experiments showed that the cutting force components were approximately independent of cutting speed. The resultant cutting force on the tool was in a direction approximately normal to the cutting face of the tool. The magnitude of the resultant force increased with the negative rake angle. Photographs of ice-chip formation revealed continuous and segmented chips at different cutting depths.

**RÉSUMÉ.** Expérience sur le travail à la machine de la glace aux angles négatives de raclage. Les composantes de la force coupante, et le moment de coupe de l'outil tranchant ont été mesurés dans des essais en machine orthogonale. Les variables comprennent la profondeur de coupe ( $< 1$  mm), la vitesse de coupe ( $0,01 \text{ m s}^{-1}$  à  $1 \text{ m s}^{-1}$ ) et les angles de raclage ( $-15^\circ$  à  $-60^\circ$ ). Les résultats des expériences ont montré que les composantes de la force de coupe était approximativement indépendante de la vitesse de coupe. La force de coupe résultante sur l'outil était dans une direction approxi-

mativement normale à la face coupante de l'outil. L'ordre de grandeur de la force résultante s'accroît avec l'angle négatif de raclage. Des photographies de la formation de copeaux de glace montrent l'existence de copeaux continus et de copeaux segmentés à différentes profondeurs de coupe.

**ZUSAMMENFASSUNG.** Versuche bei der Bearbeitung von Eis mit negative Anstellwinkeln. Die Komponenten der Schnittkraft und das Schnittmoment am Schneidwerkzeug wurden in orthogonalen Bearbeitungsversuchen gemessen. Als Variable wurden die Schnitttiefe ( $< 1$  mm), die Schneidgeschwindigkeit ( $0,01 \text{ m s}^{-1}$  bis  $1 \text{ m s}^{-1}$ ) und die Anstellwinkel ( $-15^\circ$  bis  $-60^\circ$ ) eingeführt. Die Versuchsergebnisse zeigten, dass die Komponenten der Schnittkraft annähernd unabhängig von der Schneidgeschwindigkeit waren. Die resultierende Schnittkraft am Werkzeug war ungefähr senkrecht zur Schnittfront des Werkzeugs gerichtet. Die Grösse der Resultante wuchs mit dem negativen Anstellwinkel. Photographien der Eisspanbildung zeigten fortlaufende und unterbrochene Späne bei verschiedenen Schnitttiefen.

## NOMENCLATURE

- $\beta$  = edging angle; the acute angle between the cutting face of the tool and the surface of the ice:  
 $\beta = \pi/2$  minus the rake angle.
- $f_n$  = cutting force component normal to the plane surface of the specimen per unit tool width.
- $f_t$  = cutting force component tangential to the plane surface of the specimen per unit tool width.
- $l$  = depth of tool penetration into the ice.
- $v$  = cutting speed.

## INTRODUCTION

The mechanics of ice is of practical interest whenever cutting or boring of the material is required. The management and removal of ice and snow, the building of structures surrounded by moving ice, the formation of ice structures, and the mechanics of skiing and skating involve the machining of ice. Understanding ice cutting in skiing was the principal motivation for this work. Cutting in skiing occurs during turning maneuvers; the ski cuts the snow and ice at a negative rake angle. Because ice is a brittle solid at temperatures typically near its melting point in skiing, phase transformation often occurs during cutting.

The material properties of ice have been reported by Mellor (1980) and Glen (1975), and the fracture of ice under impact loads was studied by Liu and Miller (1979). There is an indication in the literature that cutting forces in the machining of ice are independent of tool speed. Mellor (1977) showed the independence of cutting force from cutting speed in rock and ceramic machining. Brown (1979) and Hawkes and Mellor (1972) reported that the failure stress of ice in tension was relatively independent of strain-rate above about  $10^{-6} \text{ s}^{-1}$ .

The problem addressed in these experiments is the dependence of the tool forces  $f_t$  and  $f_n$  in Figure 1

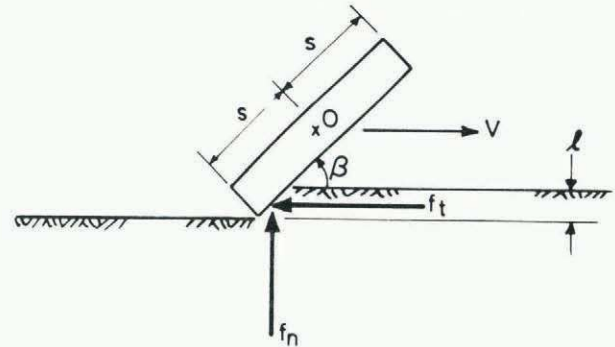


Fig. 1. Schematic of machining experiments.

upon the depth of penetration  $l$ , the edging angle  $\beta$ , and the cutting speed  $v$  in a parallel, orthogonal machining process. Because the mechanics of ice cutting is unknown, this dependence cannot be predicted from cutting theories or from tabulated data on the strength and material properties of ice. A test apparatus was developed to measure the tool forces for ice cutting with tools at negative rake angles. Cutting speeds between  $0.01 \text{ m s}^{-1}$  and  $1 \text{ m s}^{-1}$  and penetration depths of less than  $1 \text{ mm}$  were tested. The tool forces were found to be independent of tool speed in the speed range investigated. Photographs of ice chip formation of each test revealed two distinct chip types at shallow and deep penetration depths.

## EQUIPMENT SET-UP

Ice specimens were prepared from local tap water that was boiled for a minimum of 30 min to reduce the dissolved air. The specimen molds were  $50 \times 80 \times 140 \text{ mm}^3$  metal trays fitted with acrylic inserts to form the cutting surface of the specimens to a particular shape. Each mold was externally insulated with polyurethane foam on the top and sides only.

This insulation caused the specimens to freeze progressively from the bottom to the top. Thus residual stresses locked into the solidifying ice were minimized, and cracking of the specimens during preparation was eliminated. The molds were coated with silicone grease to facilitate specimen removal.

The specimen geometry included a 44 x 80 x 130 mm<sup>3</sup> base block with two raised sample volumes upon which the cutting was performed. The sample volume thickness x width x length was 6 x 38 x 40 mm<sup>3</sup> in the majority of the tests. A 6 x 50 x 40 mm<sup>3</sup> sample volume was cut to investigate the importance of sample width on the cutting force per unit sample width. Ice in the sample volumes was uniform with an average gas-bubble diameter of approximately 20 μm and a bubble density of approximately 2-3/mm<sup>3</sup>. The specimens were mounted on a grooved aluminum base plate by partially melting the base block into the grooves and then refreezing the assembly.

The cutting tool was aluminum with an inserted steel cutting edge at the tip of dimensions 8 x 60 x 40 mm<sup>3</sup> hardened to BHN 500. The cutting edge was sharpened by grinding the relief face. The tool was defined as "sharp" if there were no visible edge defects under a magnification of 30x. An aluminum fixture held the tool at a specified edging angle β as illustrated in Figure 1. The total mass of the tool and tool holder assembly was 0.113 kg.

The cutting forces were measured with a ring-type, strain-gage dynamometer. Three full strain-gage bridges measured the vertical and horizontal forces and the moment normal to the plane of these forces at point 0 in Figure 1. The resolution of the transducer was ±5 N in the range 0-400 N for any force in the t-n plane. The transducer compliance was linear at 0.098 μm N<sup>-1</sup> for horizontal forces, 1.03 μm N<sup>-1</sup> for vertical forces, and 2.6 mrad N<sup>-1</sup> m<sup>-1</sup> for torsional transducer loads. The external dimensions of the transducer were 10 x 125 x 70 mm<sup>3</sup> and the total mass was 0.39 kg.

The transducer-tool assembly was driven with a linear hydraulic actuator system (MTS model 204.51) with a 14 700 N force capacity and a 150 mm maximum stroke length. Reference signals for constant-velocity tool motion were output by a digital function generator. Position feedback of the actuator for the controller was provided by a LVDT on the actuator piston. The specimen was clamped to an adjustable table to position the height of the specimen relative to the cutting edge of the tool.

The specimens were cut inside a 610 x 710 x 610 mm<sup>3</sup> chamber maintained at -5°C ± 1.5 deg. More precise temperature control was not found necessary from the consistency and reproducibility of the data. The cutting processes were observed and photographed through windows on the top and sides of the chamber positioned normal to the cutting direction.

The horizontal and vertical force components, the moment, and the actuator position data were recorded with a transient waveform recorder (Biomation mode 1015) with a 10 bit A/D converter and a 1024 word record length per channel. The four channels were sampled simultaneously at least 500 times during the cutting phase of a test. A pre-trigger mode in the recorder permitted viewing of the data before and after contact of the cutting edge and the specimen. Recording was triggered by the transducer moment signal. Blocking of the data, and all data calibration and reduction were performed on a PDP-8E mini-computer system.

#### EXPERIMENTAL PROCEDURE

A surface preparation procedure assured uniform cutting across the entire specimen width. Each specimen was clamped to the adjustable table and

raised until the cutting edge of the tool just contacted the specimen surface. Facing of the specimen surface was performed by cutting on the forward and backward tool strokes at 76 mm s<sup>-1</sup>, raising the specimen 25.4 μm before each forward cut. This facing operation continued approximately 20 times so that the entire original surface of the specimen was machined to some extent. The specimen surface preparation was completed by continuing with an additional 20 forward and 20 backward strokes without changing the specimen height. The final specimen surface was smooth and flat, and it gave a high-quality reflective image.

The height of the specimen was measured at the beginning of each test with a dial indicator graduated to 12.7 μm. A 1 mm thick aluminum plate was used to protect the sample surface from the foot of the dial indicator. The cutting tool was then moved into the starting position, and the cutting height was adjusted by raising the specimen relative to the tool. Immediately after the single forward stroke test, ice cuttings were "lightly" brushed from the sample surface and the specimen height was measured again. The difference between the two measurements was the measure of the cutting depth. Approximately 10% of all tests were discarded due to sample chipping or cracking. Following the test, the specimen was refaced, as described above, and used in subsequent tests if sufficient sample surface remained.

Specimens brought directly from the storage freezer resided in the test chamber for a minimum of one hour prior to facing and testing to allow the temperature to reach approximate equilibrium. No significant tool wear was observed over the entire course of the experiments.

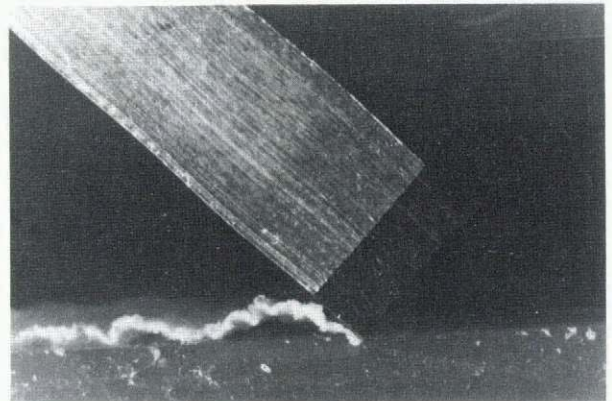


Fig.2. Continuous ice chip. β = 45°, l = 38 μm, v = 15 mm s<sup>-1</sup>.

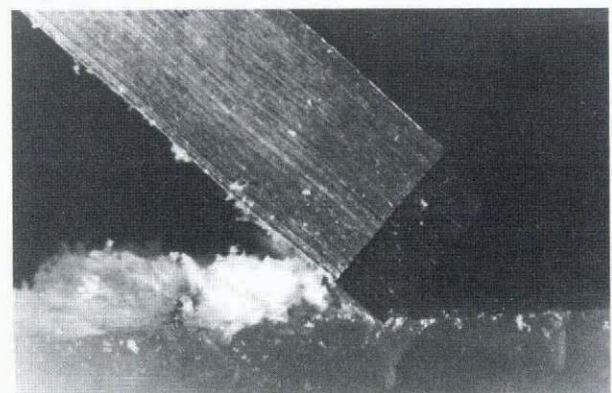


Fig.3. Segmented ice chip. β = 45°, l = 200 μm, v = 15 mm s<sup>-1</sup>.

TABLE I. FORCE AND MOMENT REPEATABILITY  
 $v = 15 \text{ mm s}^{-1}$ ,  $\beta = 45^\circ$ 

Test No.	Sample No.	$l$ $\mu\text{m}$	$f_x$ $\text{N m}^{-1}$	$f_y$ $\text{N m}^{-1}$	$M_z$ $\text{N m}^{-1}$
1	1	200	3946	3969	176
2	1	200	4050	4075	181
3	1	200	4019	4001	177
4	2	200	3886	3983	175
5	2	200	3990	4006	178
6	2	200	4093	3987	178
7	2	200	4065	4039	179
8	2	200	4095	4047	180
9	3	200	4025	4012	178
10	3	200	4072	4016	179
11	4	200	4142	4152	184
12	4	200	4304	4278	189
13	5	38	1999	2074	92.7
14	5	38	1932	2010	89.7
15	5	38	1954	1983	88.8
16	6	38	1877	1903	85.8
17	6	38	1806	1861	83.5
18	7	38	1851	1951	86.2
19	7	38	1793	1858	82.6
20	7	38	1904	1925	86.2
21	8	38	1852	1854	83.6
22	8	38	1852	1862	83.3

## RESULTS AND DISCUSSION

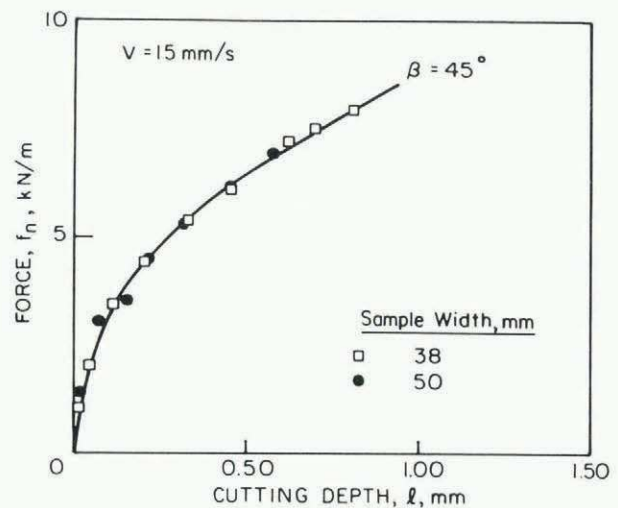
The force and moment repeatability for tests within a single sample and between different samples was addressed first. 22 tests with an edging angle ( $\pi/2$  minus rake angle) of  $\beta = 45^\circ$ , a sample width of 38 mm, and a cutting speed of  $v = 15 \text{ mm s}^{-1}$  were conducted and the results are summarized in Table I. The cutting depths were  $l = 200 \mu\text{m}$  in twelve tests on four samples and  $38 \mu\text{m}$  in ten tests on four samples. The two cutting depths produced different types of chips, representing different failure processes. At  $l = 38 \mu\text{m}$ , the chip was continuous and well defined as shown in Figure 2. The standard deviation of the cutting forces and moment within each test was approximately 5% of the mean. At  $l = 200 \mu\text{m}$ , the chip was formed by distinct, segmented ice particles as shown in Figure 3. The chip was often discontinuous with ice particles spraying out in front of the tool and with cracks forming in the ice beneath the tool. Tool chatter was more pronounced in this case and the standard deviations of the cutting forces were approximately 10% of the mean.

The maximum deviation of the mean forces and moment for each test from the averages of these means was +6% and -5% at  $l = 39 \mu\text{m}$  and +6% and -3% at  $l = 200 \mu\text{m}$ . The standard deviations of the mean forces and moments were 3% of the means at both cutting depths. Reference to cutting force or moment in the remainder of the paper denotes the mean cutting force or moment for the specified test.

The importance of specimen width on the measured loading was evaluated by comparing the curves obtained for the cutting force versus cutting depth at specimen widths of 38 mm and 50 mm at cutting depths less than 1 mm. The edging angle and cutting speed were  $\beta = 45^\circ$  and  $v = 15 \text{ mm s}^{-1}$ , respectively. The maximum deviation of the 50 mm specimen force data from the "best fit" curve drawn through the data points of the 38 mm sample was 5%, as shown in Figures 4 and 5. No apparent differences in chip

formation were observed. Specimen width or edge effects were therefore concluded to have a negligible effect on the measurements of force per unit specimen width recorded with the  $38 \mu\text{m}$  specimen.

The dependence of the cutting forces on the cutting speed was examined with tests at seven cutting speeds at two cutting depths. In the speed range investigated,  $0.01 < v < 1.0 \text{ m s}^{-1}$ , the cutting forces were approximately independent of cutting speed, as shown in Figures 6 and 7. The standard deviations of the forces at all cutting speeds was 3% of the mean at  $l = 200 \mu\text{m}$  and 5% of the mean at  $l = 38 \mu\text{m}$ . The dominant data variation associated with increased cutting speed, was increased tool chatter. The influence of the mechanical compliance in the experimental design on chatter was not investigated.

Fig. 4. Dependence of force  $f_n$  upon cutting depth.

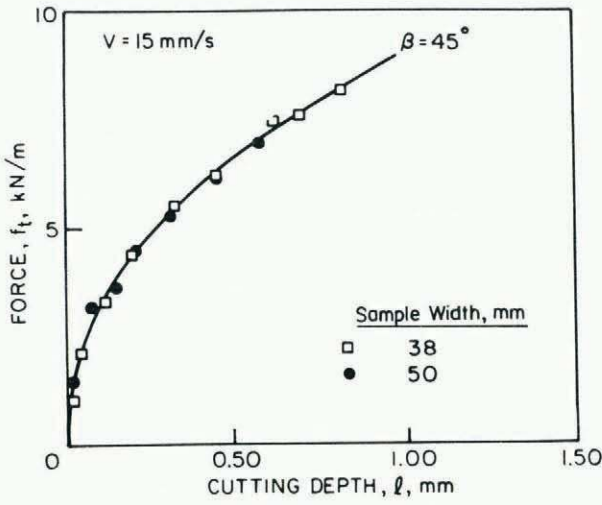


Fig.5. Dependence of force  $f_t$  upon cutting depth.

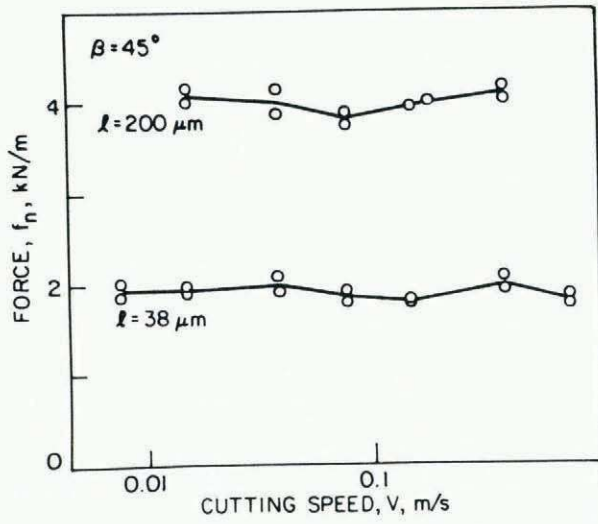


Fig.6. Dependence of force  $f_n$  upon cutting speed.

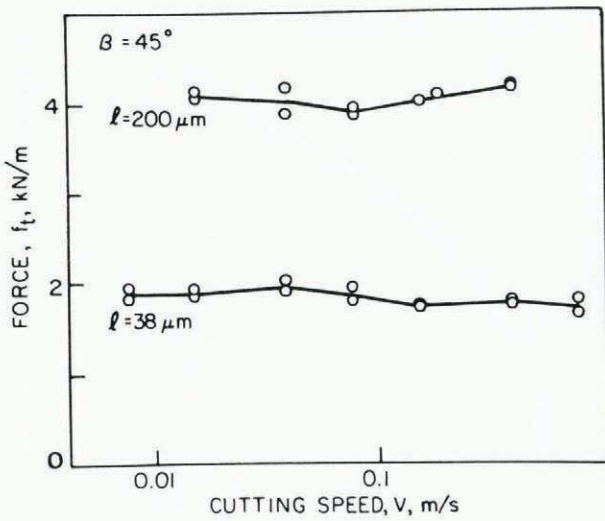


Fig.7. Dependence of force  $f_t$  upon cutting speed.

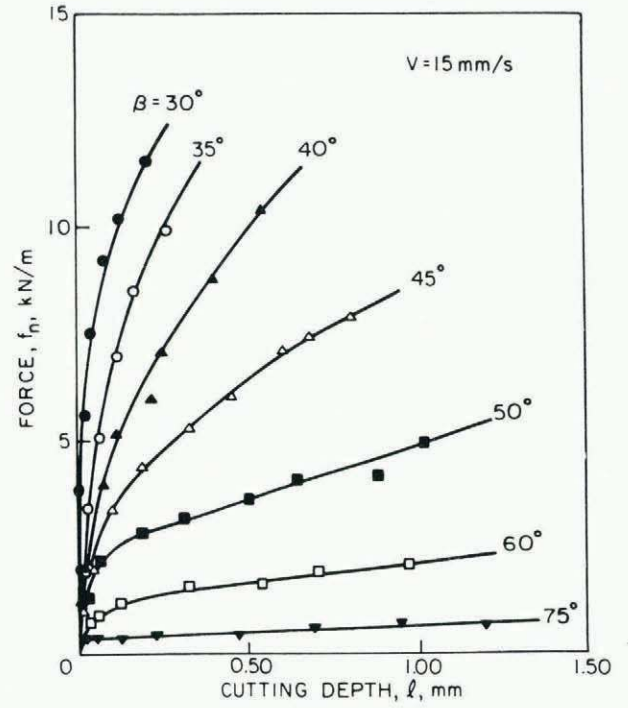


Fig.8. Dependence of force  $f_n$  upon edging angle.

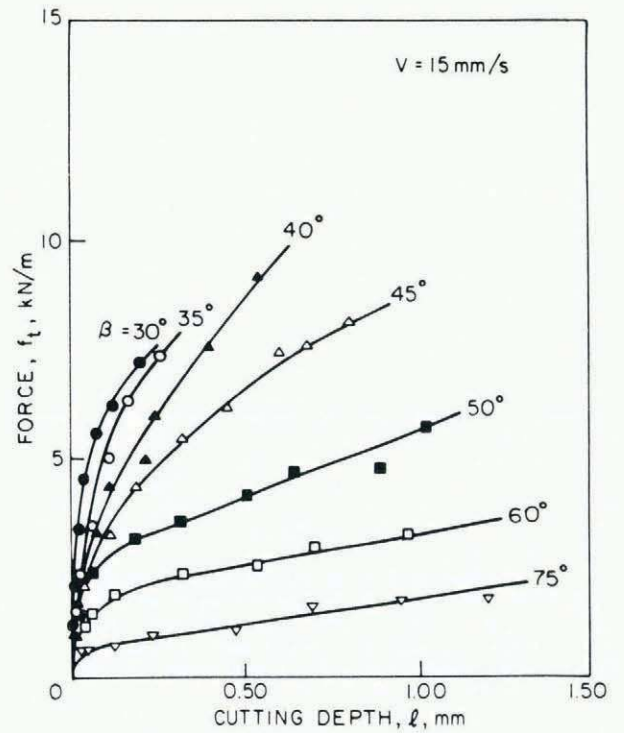


Fig.9. Dependence of force  $f_t$  upon edging angle.

TABLE II. DIRECTION OF THE RESULTANT FORCE  
Cutting speed = 15 mm s<sup>-1</sup>

$\beta = 30^\circ$		$\beta = 35^\circ$	
$z$	$\tan^{-1}f_n/f_t$	$z$	$\tan^{-1}f_n/f_t$
mm	deg	mm	deg
0.005	31.3	0.015	38.8
0.010	28.9	0.025	35.0
0.025	30.8	0.064	34.3
0.038	31.2	0.114	35.7
0.076	31.5	0.165	36.7
0.127	31.1	0.254	36.5
0.203	31.7		
$\beta = 40^\circ$		$\beta = 45^\circ$	
$z$	$\tan^{-1}f_n/f_t$	$z$	$\tan^{-1}f_n/f_t$
mm	deg	mm	deg
0.006	40.0	0.013	44.4
0.019	39.2	0.038	46.1
0.076	39.6	0.102	43.7
0.114	40.2	0.190	44.8
0.216	40.4	0.318	45.7
0.241	40.1	0.444	45.6
0.394	41.0	0.610	46.2
0.546	41.2	0.800	45.9
$\beta = 50^\circ$		$\beta = 60^\circ$	
$z$	$\tan^{-1}f_n/f_t$	$z$	$\tan^{-1}f_n/f_t$
mm	deg	mm	deg
0.025	48.8	0.038	57.5
0.064	47.7	0.057	58.5
0.183	48.3	0.127	57.0
0.311	48.4	0.318	56.6
0.508	48.7	0.546	57.5
0.648	48.9	0.711	57.4
0.876	49.0	0.965	57.8
1.020	49.3		
$\beta = 75^\circ$			
$z$	$\tan^{-1}f_n/f_t$		
mm	deg		
0.025	63.0		
0.051	63.2		
0.127	65.5		
0.229	67.3		
0.470	68.3		
0.698	67.5		
0.940	68.0		
1.210	69.7		

Eight edging angles  $\beta$  between  $30^\circ$  and  $75^\circ$  were tested at cutting depths of  $10\ \mu\text{m}$  and greater as shown in Figures 8 and 9. The cutting depth was increased until either the resultant cutting force on the tool exceeded 500 N or significant chipping and cracking of the specimen occurred. Both the force components increased with cutting depth and decreased with edging angle. At  $\beta = 45^\circ$ , the horizontal and vertical force component dependence upon cutting depth was essentially identical, indicating normality of the resultant force to the contact surface of the tool. For  $\beta$  greater (less) than  $45^\circ$  the horizontal force component was always greater (less) than the vertical component at all cutting depths.

At cutting depths less than approximately  $150\ \mu\text{m}$ , the chip was of the continuous type. For depths less than approximately  $25\ \mu\text{m}$ , the chip was also transparent. At cutting depths greater than approximately  $150\ \mu\text{m}$  the chip was discontinuous. The transition depth at  $150\ \mu\text{m}$  was not obviously dependent upon edging angle. The standard deviations of the transducer signals increased from a minimum of 5% of the mean at the shallowest cutting depth to a maximum of 12% of the mean at the deepest cutting depth.

The resultant cutting force on the tool was always approximately perpendicular to the cutting face of the tool under all test combinations. The deviation in angle of the resultant force from the normal to the tool face was within 4% except at  $\beta = 75^\circ$  where the maximum difference was 15%; see Table II. A low friction interface at the tool-ice contact, probably produced by pressure and friction melting of the ice is indicated.

## ACKNOWLEDGEMENT

The authors thank Ms Carol Brodersen for her assistance with preparation of the manuscript.

## REFERENCES

- Brown, R.L. 1979. A volumetric constitutive law for snow subjected to large strains and strain rates. *CRREL Report* (Hanover, N.H.) 79-20.
- Glen, J.W. 1975. The mechanics of ice. U.S. Cold Regions Research and Engineering Laboratory. *Cold regions science and engineering*. Hanover, N.H., Pt. II, Sect. C2b.
- Hawkes, I., and Mellor, M. 1972. Deformation and fracture of ice under uniaxial stress. *Journal of Glaciology*, Vol. 11, No. 61, p. 103-31.
- Liu, H.W., and Miller, K.J. 1979. Fracture toughness of fresh-water ice. *Journal of Glaciology*, Vol. 22, No. 86, p. 135-43.
- Mellor, M. 1977. Mechanics of cutting and boring. Part IV: dynamics and energetics of parallel motion tools. *CRREL Report* (Hanover, N.H.) 77-7.
- Mellor, M. 1980. Mechanical properties of polycrystalline ice. (In Tryde, P., ed. *International Union of Theoretical and Applied Mechanics. Physics and mechanics of ice. Symposium Copenhagen, August 6-10, 1979. Technical University of Denmark*. Berlin, etc., Springer-Verlag, p. 217-45.)

MS. received 8 March 1983 and in revised form 18 May 1983